

CERN-EP-2022-171  
08 August 2022

## Measurements of groomed-jet substructure of charm jets tagged by $D^0$ mesons in proton–proton collisions at $\sqrt{s} = 13$ TeV

ALICE Collaboration

### Abstract

Understanding the role of parton mass and Casimir colour factors in the quantum chromodynamics parton shower represents an important step in characterising the emission properties of heavy quarks. Recent experimental advances in jet substructure techniques have provided the opportunity to isolate and characterise gluon emissions from heavy quarks. In this work, the first direct experimental constraint on the charm-quark splitting function is presented, obtained via the measurement of the groomed shared momentum fraction of the first splitting in charm jets, tagged by a reconstructed  $D^0$  meson. The measurement is made in proton–proton collisions at  $\sqrt{s} = 13$  TeV, in the low jet transverse-momentum interval of  $15 \leq p_{\text{T}}^{\text{jet ch}} < 30$  GeV/ $c$  where the emission properties are sensitive to parton mass effects. In addition, the opening angle of the first perturbative emission of the charm quark, as well as the number of perturbative emissions it undergoes, are reported. Comparisons to measurements of an inclusive-jet sample show a steeper splitting function for charm quarks compared to gluons and light quarks. Charm quarks also undergo fewer perturbative emissions in the parton shower, with a reduced probability of large-angle emissions.

arXiv:2208.04857v1 [nucl-ex] 9 Aug 2022

In hadronic collisions, quarks and gluons (partons) with high transverse momentum ( $p_T$ ) and/or large masses are produced in scattering processes involving large momentum transfers. These energetic partons lose their large initial virtuality by emitting partons in a cascade process known as a parton shower, until they eventually form hadrons. Theoretical descriptions of parton showers rely on determining the emission probability of partons, which are described by splitting functions [1, 2]. Splitting functions are universal properties of quantum chromodynamics (QCD) that describe how the energy of a parton is shared as it fragments into further partons. The splitting functions of light-flavour (up, down and strange) quarks and gluons differ due to their different Casimir colour factors [2]. For heavy-flavour (charm and beauty with masses of  $(1.27 \pm 0.02) \text{ GeV}/c^2$  and  $4.18^{+0.03}_{-0.02} \text{ GeV}/c^2$ , respectively [3]) quarks the splitting functions are strongly influenced by the large quark mass [4]. As a consequence, the radiation pattern of the parton shower depends on the type of initiating parton.

Experimental access to the parton shower can be gained via measurements involving jets, which are collimated bunches of hadrons resulting from the fragmentation of partons scattered in the initial stages of collisions. Jets represent a powerful tool for testing perturbative QCD, as their inner structure (substructure) reflects the properties of the underlying parton shower. Measurements of jet substructure have been performed in inclusive jets (with no flavour tagging) to constrain the splitting functions of light quarks and gluons [5–8]. However, an experimentally clean separation of gluon-initiated and quark-initiated jets has remained challenging, with measurements constraining the splitting functions comprising an admixture of the two subsets.

Recent experimental advances in techniques pertaining to the substructure of heavy-flavour jets [9, 10] have allowed for the isolation and study of gluon emissions from heavy quarks. This technique has been used to perform a first direct measurement [11] of the dead-cone effect [12] in charm-quark jets. The dead cone corresponds to an angular region along the flight direction of the emitter, with an opening proportional to the ratio of mass to energy of the emitter, within which the probability of emissions is suppressed. The significant size of this region for low-energy heavy-flavour quarks gives rise to mass-dependent effects in the parton shower. In addition to the sensitivity to these mass effects in QCD, heavy-flavour jets represent an experimentally enhanced quark-initiated jet sample, which can be further used to constrain the flavour-dependent properties of QCD emissions arising from different Casimir colour factors.

In this work, the first measurement directly constraining the charm-quark splitting function is reported. This requires access to perturbative splittings (the splitting scale is much larger than the QCD scale) of the charm quark, where the shared momentum fraction of the splittings maps onto the analytical splitting function [13–15]. Additionally, measurements of the opening angle of these emissions, as well as the number of perturbative emissions in charm jets, are reported. Measurements of these two observables have also been reported for inclusive jets [6–8, 16, 17], with the opening angle calculated at next-to-leading logarithmic accuracy [18]. The measurements reported in this work are made in the low jet transverse-momentum interval of  $15 \leq p_T^{\text{jet ch}} < 30 \text{ GeV}/c$ , where mass effects are expected to play a role in the fragmentation of the charm quark and the inclusive sample is mainly comprised of gluon-initiated jets.

Once jets have been identified from the sample of charged particles (reconstructed as tracks) in pp collisions, using the anti- $k_T$  algorithm [19], track-based jet-substructure observables can be constructed from the jet constituents. To reconstruct the chain of emissions (splitting tree) inside a jet, the jet constituents can be reclustered with the Cambridge–Aachen (C/A) algorithm [20], which is well suited to jet substructure studies because it follows the angular ordering of emissions in QCD [1] by clustering the jet constituents based on their angular distance. By following a branch along the splitting tree returned by the reclustering procedure, a sequence of emissions can be studied [21].

Charm jets are identified by the presence of a reconstructed  $D^0$  meson amongst their constituents. The full reconstruction of the  $D^0 \rightarrow K^- \pi^+$  decay allows for the replacement of the  $D^0$  decay products with the four-momentum of the  $D^0$  meson, prior to jet clustering. This ensures that the full  $D^0$ -meson momentum is contained within the jet cone. As the charm flavour is conserved throughout the jet evolution, the charm quark can be traced as it dynamically evolves in the showering process, by following the branch containing the  $D^0$  meson through the splitting tree [9].

To reduce the contribution of non-perturbative effects and increase sensitivity to perturbative emissions [22], the Soft Drop grooming procedure [23] is applied, which only selects particular splittings of interest along the followed branch. To do this, each splitting along this branch is tested against the Soft Drop condition, as given by

$$z \equiv \frac{\min(p_{T,1}, p_{T,2})}{p_{T,1} + p_{T,2}} > z_{\text{cut}} \left( \frac{\Delta R_{1,2}}{R} \right)^\beta, \quad (1)$$

where  $p_{T,1}$  and  $p_{T,2}$  are the transverse momenta of the leading and subleading prongs of the splitting, respectively, and  $R$  is the jet resolution parameter. The grooming behaviour is determined by the parameters  $z_{\text{cut}}$  and  $\beta$ , which control the interplay between the shared momentum fraction,  $z$ , and the aperture angle between the prongs,  $\Delta R_{1,2} \equiv \sqrt{(y_1 - y_2)^2 + (\varphi_1 - \varphi_2)^2}$ , where  $y$  and  $\varphi$  are the rapidity and azimuth of prongs 1 and 2, respectively. In this work, values of  $z_{\text{cut}} = 0.1$  and  $\beta = 0$  are chosen, such that the Soft Drop condition is satisfied if the subleading prong carries at least 10% of the sum of the transverse momenta of the prongs, enriching the selection with perturbative splittings.

Two groomed substructure observables are constructed against the first splitting that satisfies the Soft Drop condition:  $z_g = z$  and  $R_g = \Delta R_{1,2}$ , as given in Eq. 1. For the given choices of grooming parameters, the shared momentum fraction,  $z_g$ , converges to the QCD splitting function at sufficiently high jet energies [13]. As the emissions are angular ordered, the groomed emission angle  $R_g$  characterises the widest emission in the splitting tree which passes the Soft Drop condition and sets the geometrical scale of the jet. This observable is expected to be sensitive to the dead cone of the charm quark at small angles, whilst emissions from gluons, which have a larger Casimir colour factor, are expected to dominate the large-angle region [24, 25]. The number of emissions of the charm quark satisfying the Soft Drop condition,  $n_{\text{SD}}$ , is also measured by evaluating all splittings along the branch containing the  $D^0$  meson. This strongly correlates to the number of perturbative emissions of the charm quark. The data were collected using the ALICE apparatus at the LHC, during the years 2016, 2017, and 2018. Information about the detector configuration and performance can be found in Refs. 26, 27. The main detector systems used for this work were the central-barrel detectors, located at  $|\eta| < 0.9$  within a solenoidal magnet and used for charged-particle tracking and identification. These include the Inner Tracking System, the Time Projection Chamber, and the Time-Of-Flight detector. The V0 detector, consisting of two scintillator arrays located at pseudorapidities of  $2.8 < \eta < 5.1$  and  $-3.7 < \eta < -1.7$ , was used for the trigger and event selections. Minimum-bias events were selected by requiring a signal above a given threshold in both V0 counters. The analysed data sample consisted of about  $1.7 \times 10^9$  pp collisions at a centre-of-mass energy of  $\sqrt{s} = 13$  TeV, corresponding to an integrated luminosity of  $\mathcal{L}_{\text{int}} = 29 \text{ nb}^{-1}$ .

The  $D^0$  mesons were reconstructed in the  $D^0 p_T$  interval of  $5 \leq p_T^{D^0} < 30 \text{ GeV}/c$ , through the  $D^0 \rightarrow K^- \pi^+$  (and charge conjugate) decay channel with a branching ratio of  $(3.95 \pm 0.03)\%$  [3]. Background candidates, built from pairs of tracks not corresponding to a  $D^0$  decay, were suppressed by applying geometrical selections on the displaced decay-vertex topology, as well as particle identification on the decay-particle tracks [28]. The  $D^0$  decay daughters were replaced in the event by the  $D^0$ -meson four-momentum, which was obtained by summing the four-momenta of these decay daughters. Jet finding was then performed using the FastJet package [29], with the anti- $k_T$  algorithm, a resolution parameter of  $R = 0.4$  and the  $E$ -scheme recombination. The inputs to the jet finder consisted of tracks of charged particles with  $p_T \geq 0.15 \text{ GeV}/c$  and the reconstructed  $D^0$ -meson candidate. The full set of quality selections applied to the tracks, including the  $D^0$ -meson candidate decay tracks, is given in Ref. 30. The

jets were required to be fully contained within the central barrel acceptance, by imposing a pseudorapidity selection of  $|\eta| < 0.5$  on the jet axis. For every  $D^0$  meson candidate in an event, jet finding was performed independently, with only the two tracks forming that particular candidate replaced with the sum of their four-momenta prior to the jet finding pass. Once jet finding had been performed, the  $D^0$ -tagged jet constituents were reclustered using the C/A algorithm and the  $z_g$ ,  $R_g$ , and  $n_{SD}$  observables were calculated for each jet. The contribution to the three observable distributions from jets tagged by background  $D^0$  candidates that survived the selection was removed via a sideband subtraction procedure, as detailed in Refs. 30, 31. This procedure provides the true  $D^0$ -tagged jet observable distributions in intervals of  $p_T^{D^0}$ .

Each of these background-subtracted distributions was scaled by the selection and reconstruction efficiency of prompt (charm-showering)  $D^0$ -tagged jets, estimated in  $p_T^{D^0}$  intervals, from Monte Carlo (MC) simulations using PYTHIA 8.243 [32–34] and GEANT 3 [35]. The efficiency-corrected distributions were summed over the full  $p_T^{D^0}$  range considered for the analysis. In order to study emissions in the charm-quark shower, the contribution from non-prompt  $D^0$  mesons, originating from the decay of beauty hadrons, was estimated using POWHEG [36] simulations with PYTHIA 6.425 [33] showering and decays implemented through the EvtGen package [37]. It was then subtracted from the measured distributions. The magnitude of this non-prompt contribution ranged from 20% to 40% in most of the  $z_g$ ,  $R_g$ , and  $n_{SD}$  intervals considered in the analysis. The  $p_T^{\text{jet ch}}$  distributions and each prompt  $D^0$ -tagged jet substructure observable were simultaneously corrected for detector effects via a two-dimensional unfolding, using the iterative Bayesian unfolding algorithm with four iterations [38].

The  $z_g$ ,  $R_g$ , and  $n_{SD}$  jet observables were also measured for inclusive jets. To allow for direct comparisons with the heavy-flavour results, the constraint on the  $Q^2$  value of the parton scattering implied by the selection of  $D^0$  mesons with  $p_T^{D^0} \geq 5 \text{ GeV}/c$  was mimicked for inclusive jets, by requiring a leading track with  $p_T \geq 5.33 \text{ GeV}/c$ . This corresponds to the  $p_T$  of a charged pion with the same transverse mass as a  $D^0$  meson with  $p_T^{D^0} = 5 \text{ GeV}/c$ . In addition, during the grooming procedure, the hardest branch of the splitting tree was followed. In the heavy-flavour sample, following the hardest branch was found to coincide with following the branch containing the  $D^0$ , in over 99% of cases. The inclusive-jet distributions were then corrected for detector effects via the same unfolding procedure as in the  $D^0$ -tagged jet case.

Systematic uncertainties related to the reconstruction and identification of prompt  $D^0$ -tagged jets were studied. The stability of the selections applied to the  $D^0$ -meson candidates were estimated by loosening and tightening the topological and PID criteria used to identify the  $D^0$  decays. The uncertainty pertaining to the signal extraction procedure was estimated by changing the fitting parameters on the invariant-mass fits, as well as the widths of the signal and sideband regions used for the sideband subtraction procedure. The uncertainty on the  $D^0$  feed-down estimation was obtained by varying the renormalisation and factorisation scales, as well as the mass of the beauty quark, in the POWHEG simulations [39]. The uncertainty on the jet energy resolution was estimated by artificially reducing the tracking efficiency used to generate the unfolding response matrix by 4%, in line with the tracking efficiency uncertainty of the ALICE detector. Finally, the uncertainty associated with the unfolding procedure was obtained by varying the number of iterations, the choice of prior, and the ranges of the response matrix. Additionally, variations of the fragmentation properties of the MC simulation used to construct the response matrix, obtained by selecting subsamples of the jets based on jet-angularity observables [40], were also included.

The dominant contributions in most of the intervals resulted from variations of the topological selections, signal extraction, and feed-down subtraction. For the feed-down subtraction uncertainty, the maximum negative and the maximum positive deviations were taken, respectively. For each of the other variation categories, the root mean square of deviations from the central values was calculated and assigned as a systematic uncertainty, which was then symmetrised around the central value. The uncertainties from all categories were then added in quadrature to obtain the full systematic uncertainty. The total systematic uncertainties range from 7% to 77%, from 9% to 12%, and from 5% to 59% for the  $D^0$ -tagged jet  $z_g$ ,  $R_g$ , and  $n_{SD}$  distributions, respectively.

The systematic uncertainties for the inclusive jet distributions were estimated by performing variations of the tracking efficiency and unfolding, in the same way as in the  $D^0$ -tagged jet case. In addition, the  $p_T$  selection on the leading track of the jet was also varied in line with the track  $p_T$  resolution of the  $D^0$ -decay tracks. The total systematic uncertainties range from 1.4% to 4.3%, from 2.2% to 5.7%, and from 3.3% to 8.1% for the inclusive jet  $z_g$ ,  $R_g$ , and  $n_{SD}$  distributions, respectively.

The first measurement mapping on to the charm-quark splitting function is reported via the  $z_g$  distribution in Fig. 1, for charm jets tagged by a prompt  $D^0$  meson. The  $R_g$  and  $n_{SD}$  distributions are shown in the left and right panels of Fig. 2, respectively. These distributions are fully corrected for detector effects and are reported in the jet transverse-momentum interval of  $15 \leq p_T^{\text{jet ch}} < 30 \text{ GeV}/c$ . Each charm-tagged jet measurement is accompanied by a measurement of an inclusive-jet sample in the same kinematic interval, also fully corrected for detector effects. Both the charm-tagged jet and inclusive jet distributions are normalised to the total number of jets in each respective category, irrespective of whether they had a splittings passing the Soft Drop condition or not. In this way, the distributions are sensitive to the proportion of jets that do not have any splittings passing the Soft Drop condition, denoted as the SD-untagged fraction. These fractions are 22% and 2.8%, in the charm-tagged jet and inclusive jet samples, respectively. Both samples are compared to PYTHIA 8 simulations and also to POWHEG + PYTHIA 6 simulations for the charm-tagged jets. The ratios of predicted distributions from parton-shower models to the measured distributions are also shown in the bottom panels of Figs. 1 and 2.

The  $z_g$  distributions show that charm-tagged jets have significantly fewer symmetric splittings (large  $z_g$  values), compared to inclusive jets. This is consistent with theoretical predictions [10] of the role of mass effects in the QCD splitting function. The  $R_g$  distribution for charm quarks shows a reduction at large-angles compared to inclusive jets. This can be due to the differences between quark and gluon fragmentation, with the gluon-dominated inclusive sample expected to feature larger-angle perturbative emissions. The charm and inclusive jet distributions are consistent at small  $R_g$ . This could be due to an interplay between the dead-cone effect, which suppresses small-angle emissions from the charm quark, and the more abundant emissions from quarks compared to gluons at small angles, as gluons lose more of their initial virtuality through larger-angle emissions. The  $n_{SD}$  distribution shows a significant shift to smaller values for the charm-tagged jets ( $\langle n_{SD} \rangle = 1.34 \pm 0.06 \text{ (stat.)} \pm 0.01 \text{ (syst.)}$ ) compared to inclusive jets ( $\langle n_{SD} \rangle = 2.31 \pm 0.01 \text{ (stat.)} \pm 0.01 \text{ (syst.)}$ ). This indicates that, compared to light and massless partons, charm quarks on average emit fewer gluons with a large enough  $p_T$  to pass the Soft Drop condition in the showering process. This is consistent with the expectation from the presence of a dead cone for charm quarks, which results in a harder fragmentation of charm quarks compared to light quarks and gluons.

For all three observables, both the PYTHIA 8 and POWHEG + PYTHIA 6 predictions for charm-quark jets describe the measurements within uncertainties. For the more precise inclusive measurements, PYTHIA 8 exhibits some tension, particularly for the  $n_{SD}$  observable. This may be partially due to the poorly constrained quark and gluon fractions in the inclusive sample at low  $p_T^{\text{jet ch}}$ . In contrast, as the  $D^0$ -tagged jets represent a quark-enriched sample, the comparison of the shower generators to data are less reliant on this fraction and can instead be used to more accurately study the mechanisms underpinning the shower properties.

The measurement of the groomed shared momentum fraction,  $z_g$ , of charm-tagged jets, reported in this letter, represents the first direct experimental constraint of the splitting function of heavy-flavour quarks. The  $z_g$  distribution appears steeper than that of light quarks and gluons, with a suppressed probability of symmetric emissions. Measurements of the number of splittings passing the Soft Drop condition as well as the emission angle of the first of these splittings, show that heavy-flavour quarks on average have fewer perturbative emissions compared to light quarks and gluons, with a lower probability of these emissions occurring at large angles. These different characteristics for heavy-quark emissions, compared to light quarks and gluons, constrain the roles of quark mass and Casimir colour factors in the parton shower,

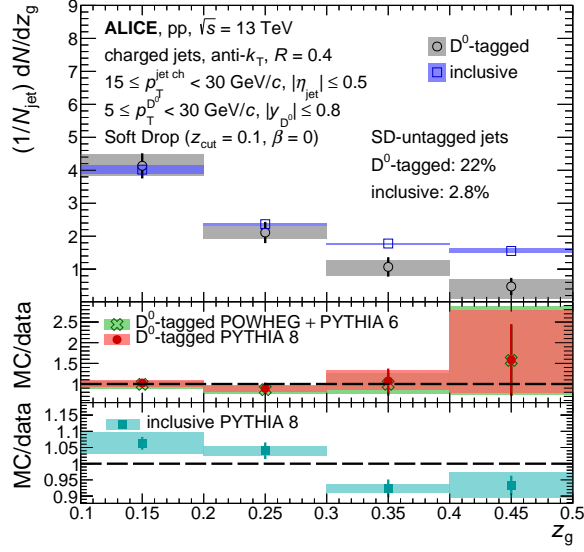


**Figure 1:** The  $z_g$  distribution of prompt  $D^0$ -tagged jets compared to that of inclusive jets for  $15 \leq p_T^{\text{jet ch}} < 30$  GeV/c in pp collisions at  $\sqrt{s} = 13$  TeV, normalised to the total number of jets. Model/data ratios are shown in the bottom panels for PYTHIA 8 [32–34] and POWHEG [36] + PYTHIA 6 [33] simulations.

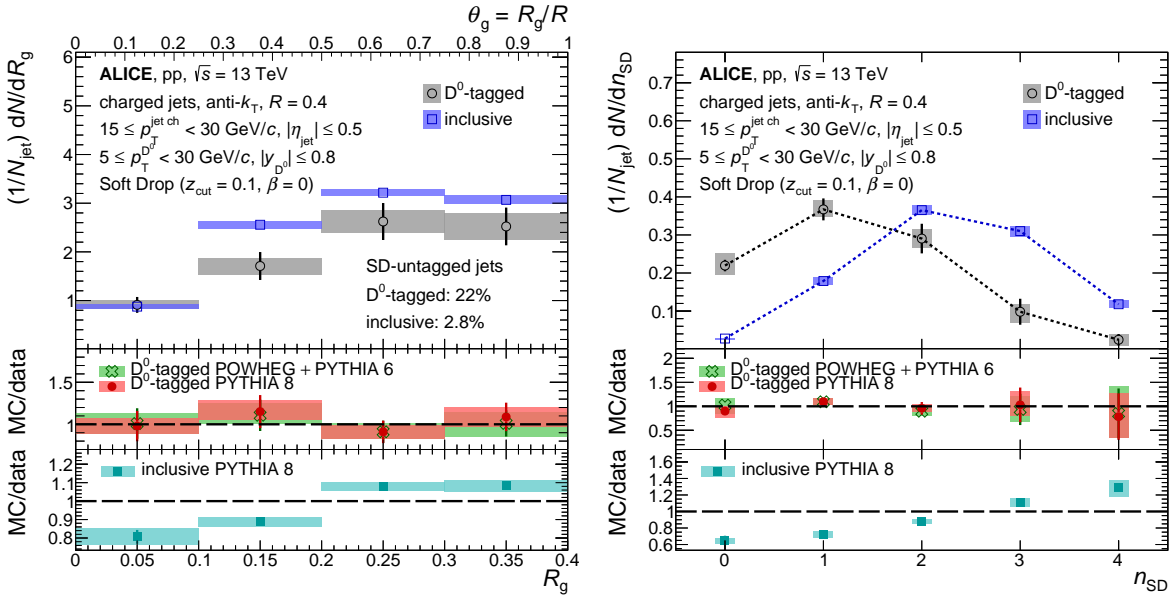


**Figure 2:** The  $R_g$  (left) and  $n_{SD}$  (right) distributions of prompt  $D^0$ -tagged jets compared to those of inclusive jets for  $15 \leq p_T^{\text{jet ch}} < 30$  GeV/c in pp collisions at  $\sqrt{s} = 13$  TeV. Model/data ratios are shown in the bottom panels for PYTHIA 8 [32–34] and POWHEG [36] + PYTHIA 6 [33] simulations.

which are different between the two samples. The upgraded ALICE detector in the LHC Run 3 will extend this measurement to jets tagged with a fully reconstructed beauty meson [41]. Direct comparison of the two quark-enriched samples of charm-tagged and beauty-tagged jets will enable the isolation of mass effects from the effects due to Casimir colour factors. The larger projected integrated luminosity in Run 3 will also allow us to extend the charm-tagged to inclusive jet comparisons to higher  $p_T^{\text{jet ch}}$ , where mass effects become negligible and the remaining impact of the Casimir colour factors can be cleanly studied.

## References

- [1] Y. L. Dokshitzer, V. A. Khoze, A. H. Mueller, and S. I. Troian, *Basics of perturbative QCD*. Ed. Frontieres, 1991.
- [2] G. Altarelli and G. Parisi, “Asymptotic freedom in parton language”, *Nuclear Physics B* **126** no. 2, (1977) 298–318.
- [3] **Particle Data Group** Collaboration, P. A. Zyla *et al.*, “Review of Particle Physics”, *PTEP* **2020** no. 8, (2020) 083C01. And 2021 update.
- [4] E. G. de Oliveira, A. D. Martin, M. G. Ryskin, and A. G. Shuvaev, “Treatment of heavy quarks in QCD”, *Eur. Phys. J. C* **73** no. 10, (2013) 2616, arXiv:1307.3508 [hep-ph].
- [5] **CMS** Collaboration, A. M. Sirunyan *et al.*, “Measurement of the Splitting Function in pp and Pb–Pb Collisions at  $\sqrt{s_{\text{NN}}} = 5.02$  TeV”, *Phys. Rev. Lett.* **120** no. 14, (2018) 142302, arXiv:1708.09429 [nucl-ex].
- [6] **ALICE** Collaboration, S. Acharya *et al.*, “Measurement of the groomed jet radius and momentum splitting fraction in pp and Pb–Pb collisions at  $\sqrt{s_{\text{NN}}} = 5.02$  TeV”, *Phys. Rev. Lett.* **128** no. 10, (2022) 102001, arXiv:2107.12984 [nucl-ex].
- [7] **ATLAS** Collaboration, G. Aad *et al.*, “Measurement of soft-drop jet observables in pp collisions with the ATLAS detector at  $\sqrt{s} = 13$  TeV”, *Phys. Rev. D* **101** no. 5, (2020) 052007, arXiv:1912.09837 [hep-ex].
- [8] **STAR** Collaboration, J. Adam *et al.*, “Measurement of groomed jet substructure observables in p+p collisions at  $\sqrt{s} = 200$  GeV with STAR”, *Phys. Lett. B* **811** (2020) 135846, arXiv:2003.02114 [hep-ex].
- [9] L. Cunqueiro and M. Płoskoń, “Searching for the dead cone effects with iterative declustering of heavy-flavor jets”, *Phys. Rev. D* **99** no. 7, (2019) 074027, arXiv:1812.00102 [hep-ph].
- [10] P. Ilten, N. L. Rodd, J. Thaler, and M. Williams, “Disentangling heavy flavor at colliders”, *Phys. Rev. D* **96** no. 5, (2017) 054019, arXiv:1702.02947 [hep-ph].
- [11] **ALICE** Collaboration, S. Acharya *et al.*, “Direct observation of the dead-cone effect in QCD”, arXiv:2106.05713 [nucl-ex].
- [12] Y. L. Dokshitzer, V. A. Khoze, and S. I. Troian, “On specific QCD properties of heavy quark fragmentation (‘dead cone’)”, *J. Phys. G* **17** (1991) 1602–1604.
- [13] A. Larkoski, S. Marzani, J. Thaler, A. Tripathy, and W. Xue, “Exposing the QCD Splitting Function with CMS Open Data”, *Phys. Rev. Lett.* **119** no. 13, (2017) 132003, arXiv:1704.05066 [hep-ph].

- [14] A. J. Larkoski, S. Marzani, and J. Thaler, “Sudakov safety in perturbative QCD”, *Phys. Rev. D* **91** no. 11, (2015) 111501, [arXiv:1502.01719 \[hep-ph\]](#).
- [15] P. Cal, K. Lee, F. Ringer, and W. J. Waalewijn, “The soft drop momentum sharing fraction  $z_g$  beyond leading-logarithmic accuracy”, [arXiv:2106.04589 \[hep-ph\]](#).
- [16] **ALICE** Collaboration, S. Acharya *et al.*, “Exploration of jet substructure using iterative declustering in pp and Pb–Pb collisions at LHC energies”, *Phys. Lett. B* **802** (2020) 135227, [arXiv:1905.02512 \[nucl-ex\]](#).
- [17] **ALICE** Collaboration, S. Acharya *et al.*, “Measurements of the groomed jet radius and momentum splitting fraction with the soft drop and dynamical grooming algorithms in pp collisions at  $\sqrt{s} = 5.02$  TeV”, [arXiv:2204.10246 \[nucl-ex\]](#).
- [18] Z.-B. Kang, K. Lee, X. Liu, D. Neill, and F. Ringer, “The soft drop groomed jet radius at NLL”, *JHEP* **02** (2020) 054, [arXiv:1908.01783 \[hep-ph\]](#).
- [19] M. Cacciari, G. P. Salam, and G. Soyez, “The anti- $k_t$  jet clustering algorithm”, *JHEP* **04** (2008) 063, [arXiv:0802.1189 \[hep-ph\]](#).
- [20] Y. L. Dokshitzer, G. D. Leder, S. Moretti, and B. R. Webber, “Better jet clustering algorithms”, *JHEP* **08** (1997) 001, [arXiv:hep-ph/9707323](#).
- [21] F. A. Dreyer, G. P. Salam, and G. Soyez, “The Lund Jet Plane”, *JHEP* **12** (2018) 064, [arXiv:1807.04758 \[hep-ph\]](#).
- [22] **ALICE** Collaboration, S. Acharya *et al.*, “Measurements of the groomed and ungroomed jet angularities in pp collisions at  $\sqrt{s} = 5.02$  TeV”, [arXiv:2107.11303 \[nucl-ex\]](#).
- [23] A. J. Larkoski, S. Marzani, G. Soyez, and J. Thaler, “Soft drop”, *JHEP* **05** (2014) 146, [arXiv:1402.2657 \[hep-ph\]](#).
- [24] **OPAL** Collaboration, P. D. Acton *et al.*, “A Study of differences between quark and gluon jets using vertex tagging of quark jets”, *Z. Phys. C* **58** (1993) 387–404.
- [25] **CMS** Collaboration, A. Tumasyan *et al.*, “Study of quark and gluon jet substructure in Z+jet and dijet events from pp collisions”, *JHEP* **01** (2022) 188, [arXiv:2109.03340 \[hep-ex\]](#).
- [26] **ALICE** Collaboration, K. Aamodt *et al.*, “The ALICE experiment at the CERN LHC”, *JINST* **3** (2008) S08002.
- [27] **ALICE** Collaboration, B. Abelev *et al.*, “Performance of the ALICE Experiment at the CERN LHC”, *Int. J. Mod. Phys. A* **29** (2014) 1430044, [arXiv:1402.4476 \[nucl-ex\]](#).
- [28] **ALICE** Collaboration, S. Acharya *et al.*, “Measurement of the production of charm jets tagged with  $D^0$  mesons in pp collisions at  $\sqrt{s} = 7$  TeV”, *JHEP* **08** (2019) 133, [arXiv:1905.02510 \[nucl-ex\]](#).
- [29] M. Cacciari, G. P. Salam, and G. Soyez, “FastJet user manual”, *Eur. Phys. J. C* **72** (2012) 1896, [arXiv:1111.6097 \[hep-ph\]](#).
- [30] **ALICE** Collaboration, S. Acharya *et al.*, “Measurement of the production of charm jets tagged with  $D^0$  mesons in pp collisions at  $\sqrt{s} = 5.02$  and 13 TeV”, [arXiv:2204.10167 \[nucl-ex\]](#).
- [31] **ALICE** Collaboration, S. Acharya *et al.*, “Groomed jet substructure measurements of charm jets tagged with  $D^0$  mesons in pp collisions at  $\sqrt{s} = 13$  TeV”, 2020. <https://cds.cern.ch/record/2719005>. ALICE-PUBLIC-2020-002.

- [32] P. Skands, S. Carrazza, and J. Rojo, “Tuning PYTHIA 8.1: the Monash 2013 tune”, *Eur. Phys. J. C* **74** no. 8, (2014) 3024, arXiv:1404.5630 [hep-ph].
- [33] T. Sjostrand, S. Mrenna, and P. Z. Skands, “PYTHIA 6.4 physics and manual”, *JHEP* **05** (2006) 026, arXiv:hep-ph/0603175.
- [34] T. Sjöstrand, S. Ask, J. R. Christiansen, R. Corke, N. Desai, P. Ilten, S. Mrenna, S. Prestel, C. O. Rasmussen, and P. Z. Skands, “An introduction to PYTHIA 8.2”, *Comput. Phys. Commun.* **191** (2015) 159–177, arXiv:1410.3012 [hep-ph].
- [35] R. Brun, F. Bruyant, M. Maire, A. C. McPherson, and P. Zancarini, *GEANT 3 : user’s guide Geant 3.10, Geant 3.11; rev. version*. CERN, Geneva, 1987.  
<https://cds.cern.ch/record/1119728>.
- [36] S. Alioli, P. Nason, C. Oleari, and E. Re, “A general framework for implementing NLO calculations in shower Monte Carlo programs: the POWHEG BOX”, *JHEP* **06** (2010) 043, arXiv:1002.2581 [hep-ph].
- [37] D. J. Lange, “The EvtGen particle decay simulation package”, *Nucl. Instrum. Meth. A* **462** (2001) 152–155.
- [38] G. D’Agostini, “A multidimensional unfolding method based on Bayes’ theorem”, *Nucl. Instrum. Meth. A* **362** (1995) 487–498.
- [39] M. Cacciari, P. Nason, and R. Vogt, “QCD predictions for charm and bottom production at RHIC”, *Phys. Rev. Lett.* **95** (2005) 122001, arXiv:hep-ph/0502203.
- [40] A. J. Larkoski, J. Thaler, and W. J. Waalewijn, “Gaining (Mutual) Information about Quark/Gluon Discrimination”, *JHEP* **11** (2014) 129, arXiv:1408.3122 [hep-ph].
- [41] ALICE Collaboration, S. Acharya *et al.*, “Future high-energy pp programme with ALICE”,  
<https://cds.cern.ch/record/2724925>. ALICE-PUBLIC-2020-005.
- [42] H. T. Li and I. Vitev, “Inverting the mass hierarchy of jet quenching effects with prompt b-jet substructure”, *Phys. Lett. B* **793** (2019) 259–264, arXiv:1801.00008 [hep-ph].
- [43] H. T. Li, Z. L. Liu, and I. Vitev, “Heavy flavor jet production and substructure in electron–nucleus collisions”, *Phys. Lett. B* **827** (2022) 137007, arXiv:2108.07809 [hep-ph].

## A Supplementary material

The measured  $z_g$  distribution is also compared to analytical calculations performed in the soft-collinear effective theory (SCET) framework with resummation to modified leading-logarithmic accuracy (MLL) [42, 43], presented in Fig. A.1, which are consistent with the data. The calculations do not include hadronisation effects and are performed utilising a leading-order evaluation of the charm cross section, which experimentally corresponds to jets with both charged and neutral information. It is expected that the low- $z_g$  region of the calculations are affected by non-perturbative effects. For comparison with the SCET predictions, the measurement is normalised to the number of jets passing the Soft Drop condition in each sample, as the calculations are provided for  $z_g \geq 0.1$  and do not include an untagged fraction.

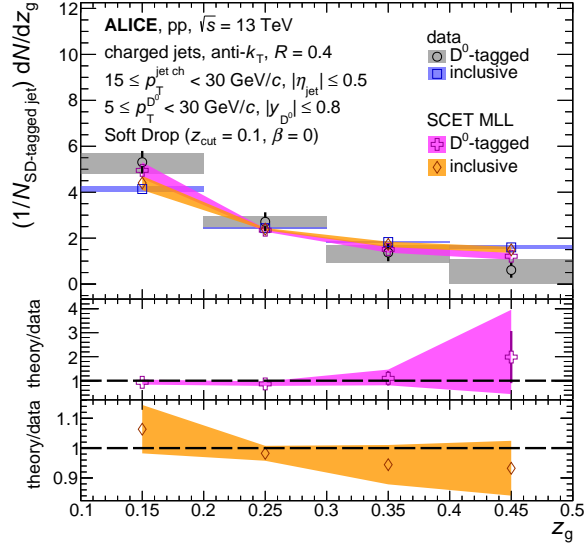


**Figure A.1:** The  $z_g$  distribution of prompt  $D^0$ -tagged jets compared to that of inclusive jets for  $15 \leq p_T^{\text{jet ch}} < 30$  GeV/c in pp collisions at  $\sqrt{s} = 13$  TeV, normalised to the number of jets passing the Soft Drop condition. Model/data ratios are shown in the bottom panels for soft-collinear effective theory calculations [42, 43].